Radially dependent solutions of Boltzmann's equation in low-temperature plasmas using a modified two-term expansion

Michael J. Hartig[a] and Mark J. Kushner[b]
University of Illinois, Department of Electrical and Computer Engineering, 1406 W. Green Street, Urbana, Illinois 61801

(Received 12 March 1992; accepted for publication 6 October 1992)

A new method for obtaining spatially resolved electron energy distributions is described and applied to cylindrical bore electric discharges. The method is based on a modified two-term spherical harmonic expansion of Boltzmann's equation in which energy-resolved drift and diffusion are included, as well as Joule heating or cooling by the ambipolar field. It is found that low-energy electrons may be heated by the large ambipolar electric field gradients near the wall while higher-energy electrons may escape the plasma. Therefore, diffusion cooling and Joule heating in the ambipolar field may simultaneously occur, but for different portions of the electron energy distribution.

I. INTRODUCTION

A widely accepted method for obtaining the electron energy distribution (EED) in partially ionized gases is to solve Boltzmann's equation using a spherical harmonic expansion.[1-3] In applications where the electron scattering is predominantly isotropic and momentum transfer is dominated by elastic collisions, solutions that retain only the first two terms in the expansion usually yield sufficiently accurate results. Higher-order expansions, retaining up to ten terms, have been used when electron scattering is anisotropic or when momentum transfer results from inelastic collisions, as may occur when vibrational or rotational excitation cross sections are large.[2] Fully resolving Boltzmann's equation in both position and velocity is a computationally intensive task. For this reason, solutions of Boltzmann's equation using spherical harmonic expansions (SHE) are almost always spatial averages.

In applications where it is either desirable or necessary to spatially resolve the EED, solutions other than the SHE are usually used. Monte Carlo simulations,[4] particle-in-cell models,[5] multibeam representations,[6] or direct integrations of Boltzmann's equation[7] have been successfully used in this regard. One can, however, use the SHE to obtain spatial information on the EED under somewhat stringent conditions. If the rate at which the EED equilibrates with the electric field is large compared to either the time or spatial frequency with which the electric field varies, then one can approximate that the EED is in equilibrium with the instantaneous local electric field, $f(\epsilon,\mathbf{r},t)=F[E/N(\mathbf{r},t)]$, where E/N is the electric-field/gas-number density. The local EED can then be obtained using a two-term SHE based on the local field,[8] a practice known as the local-field approximation (LFA).

The cylindrical positive column glow discharge is one of the most studied low-temperature plasmas.[9] Although usually analyzed as having a uniform axial electric field, there are two effects that can lead to significant variations in E/N as a function of radius. The first is volumetric gas heating which can result in rarification of the gas on the axis. This causes the E/N on the axis to be larger than the E/N near the walls. The second effect is the ambipolar space-charge field. The purpose of the space-charge field, pointing radially outward, is to retard the flux of electrons diffusing to the walls to be equal to that of the ions. Simple diffusion theory states that the ambipolar electric field E_a in positive column discharges scales roughly as $kT_e/q\Lambda$,[10] where T_e is the electron temperature and Λ is the diffusion length of the column. E_a can have values comparable to the applied axial electric field. The radial electric field has been measured by observing the Stark shift of Rydberg-excited He atoms in a positive column, and values exceeding tens of V cm^{-1} were obtained.[11]

In all cases where there is an ambipolar electric field, the magnitude of the total vector electric field exceeds that of the applied axial electric field. A number of works have attempted to account for the combined effects of the radial electric field and space-charge potential $\phi(r)$ on the electron energy distribution.[12-17] Bernstein and Holstein[12] investigated the average EED in a parallel-plate discharge where there is no loss of electrons to the wall, and hence no diffusion cooling, and where E_a is large compared to the applied axial field. They found that by including the effects of the space-charge field, the tail of the EED was enhanced and ionization rates increased, though the effect was small. This additional ionization conceptually results from electrons near the wall which are accelerated by the axial electric field to energies near to the ionization threshold. The electrons may then elastically diffuse towards the center of the discharge, thereby gaining energy in excess of the ionization potential by "falling" down the space-charge potential. This effect has been termed "diffusion heating."[18] Due to computational limitations at the time, Bernstein and Holstein were only able to obtain a spatially averaged EED while ignoring the loss of electrons to the wall. The latter assumption precludes the effects of diffusion cooling, where high-energy electrons leave the discharge at a higher rate than lower-energy electrons.

[a]Present address: Motorola, Inc., 3501 Ed Bluestein Boulevard, P. O. Box 6000, Austin, TX 78762.
[b]Author to whom correspondence should be addressed.

 0021-8979/93/031080-11$06.00

Assuming a parabolic radial potential, Tsendin and Golubovskii[16] were able to radially resolve the EED for the case $R > \lambda$, where R is the radius of the discharge tube and λ is the electron mean free path. They found that there are two energies at which the slope of the EED changes (or at which the EED is "cut off"). The first corresponds to the threshold for inelastic collisions. The second corresponds to the ambipolar potential. Electrons with an energy greater than this value are able to climb the space-charge hill and leave the plasma.

Bhattacharya and Ingold[19] calculated electron and ion temperatures in an afterglow using a hydrodynamic formulation for the heavy particles and a Maxwellian velocity for the electrons. They allowed electrons to have energies greater than the space-charge potential, and therefore reach the wall. These calculations, when compared to experimental data, revealed some evidence of diffusion cooling. Ferreira and Ricard[20] developed a model for low-pressure argon positive column discharges which also allows velocity-resolved electron losses to the wall, but the EED is taken as a spatial average. Their results show good agreement with experiment for pressures below 0.1 Torr where the electron mean free path is commensurate with the radius of the discharge tube, but the agreement is less good at pressures above that value, an effect the authors attribute to the EED being a function of radius at the higher pressure.

As mentioned above, spherical harmonic expansions are not traditionally used when the LFA cannot be applied and when spatial variations in the EED are expected. The two-term SHE is based, however, on elastic collisions dominating momentum transfer and on momentum-transfer collisions being primarily isotropic. Given this basis, one might expect that the two-term SHE can be applied to spatially resolving the EED in discharges where diffusion is the dominant form of electron transport. Based on this expectation, we have developed a method of spatially resolving an EED using the two-term SHE, and in this article we present spatially dependent solutions to Boltzmann's equation using that method. The model system is a positive column cylindrical bore discharge where the total E/N is a function of position due to the consequences of the radial space-charge field. Radial transport is accounted for by formulating a set of partial differential equations based on the local two-term SHE and adding velocity-resolved drift and diffusion. The heating, or cooling, effects of the ambipolar electric field are also included by treating the Joule heating term as a vector product of the axial and radial current densities with the axial and radial electric fields.

We find that radial electron transport significantly perturbs rate coefficients for high threshold processes compared to those values one would obtain using the LFA. Akin to the diffusion cooling effect, as studied by Biondi[21] and others,[15,19,22,23] higher-energy electrons diffuse against the space-charge field and leave the system at a faster rate than low-energy electrons. This lowers rate coefficients for high threshold processes. The effects of the ambipolar electric field are less straightforward. The dominant effect of the radial electric field is to slow the transport of the higher-energy electrons which would otherwise stream out of the plasma thereby equilibrating the total flux of electrons and ions. At the same time, low-energy electrons which are nearly in equilibrium with the local electric field see a net higher field, a consequence of the vector sum of the axial and radial components. Under these conditions, the bulk electron temperature can increase at larger radii where the total electric field is larger, while high threshold energy rate coefficients decrease because of the loss or slowing of the higher-energy electrons.

In Sec. II we describe our model while applications of the model to He/Hg plasmas and Ar/Hg plasmas are discussed in Sec. III. Comparisons to previous work are made in Sec. IV, and our concluding remarks are in Sec. V.

II. DESCRIPTION OF THE MODEL

The two-term SHE solution of Boltzmann's equation for the EED is based on the assumptions that elastic momentum-transfer collisions dominate electron transport and that the collisions are dominantly isotropic. These are conditions for which electron transport in the presence of gradients is dominated by diffusion. Given these conditions we modeled the spatially dependent EED in cylindrical glow discharges using a radially resolved two-term SHE augmented by energy-dependent drift and diffusion perpendicular to the axis. Conceptually, we solve the two-term SHE for the EED at given radial points using the local electric field at those points. The EED at each radial point is coupled by energy-resolved diffusion resulting from density gradients. By solving for the ambipolar radial electric field, energy-resolved advective transport can also be included. The local value of the radial electric field is also used in the Joule heating term of the SHE to account for heating or cooling of the electrons resulting from the ambipolar field. Although our model system is a cylindrical glow discharge, the methodology can be extended to other geometries.

Our implementation of the two-term SHE is based on the discretization method employed by Rockwood.[24] Boltzmann's equation using the two-term SHE at radial location r can be written as

$$\frac{\partial f(\epsilon,r)}{\partial t} = -\frac{\partial}{\partial \epsilon}\left[\frac{2\epsilon e^2 E(r)^2}{3m\nu(\epsilon)}\left(\frac{f(\epsilon,r)}{2\epsilon} - \frac{\partial f(\epsilon,r)}{\partial \epsilon}\right)\right] + \left(\frac{\partial f(\epsilon,r)}{\partial t}\right)_c = \left(\frac{\partial f(\epsilon,r)}{\partial t}\right)_L, \quad (1)$$

where $f(\epsilon,r)$ is the EED for energy ϵ at radius r, having units $\mathrm{cm}^{-3}\,\mathrm{eV}^{-1}$, and $\nu(\epsilon)$ is the collision frequency for momentum transfer. In Eq. (1) the first term on the right-hand side accounts for Joule heating from the applied axial field E, while the second term accounts for elastic and inelastic collisions, both with the gas and with other electrons. The collision term depends only on local values of $f(\epsilon,r)$ and on the local density of collision partners. Since this term does not directly affect radial electron transport, and our implementation of the collision term (including

electron-electron collisions) is identical to that of Rockwood,[24] we will not describe it further. When considering only local effects in solving Boltzmann's equation, the terms in Eq. (1) are adequate for the analysis. To denote this condition, we use the subscript L.

To spatially resolve the EED, additional terms to Eq. (1) must be considered. To include radial transport, we modified Eq. (1) to

$$\frac{\partial f(\epsilon,r)}{\partial t}=\left(\frac{\partial f(\epsilon,r)}{\partial t}\right)_L+\nabla_r\cdot[D(\epsilon,r)\cdot\nabla_r f(\epsilon,r)+\mu(\epsilon,r)\cdot\mathbf{E}_a(r)f(\epsilon,r)], \tag{2}$$

with the direction of the ambipolar field $\mathbf{E}_a$ defined as being positive when pointing away from the axis. When the transport terms are averaged over the EED, one obtains the conventional expression for space-charged-limited transport, $\nabla_r\cdot(D_a\cdot\nabla_r n_e)$, where D_a is the ambipolar diffusion coefficient. The exceptional points of Eq. (2) are that by energy resolving the advective and diffusive transport, different portions of the EED may be dominantly affected by different modes of transport. For example, E_a is determined in large part by the transport coefficients of the more numerous low-energy electrons which have large momentum-transfer cross sections. E_a may not be large enough, however, to confine more mobile higher-energy electrons. Diffusion will therefore dominate the latter group's transport. Conversely, highly collisional electrons that are in strict equilibrium with the local electric field may, in fact, convect radially inward in response to the ambipolar field and be heated to higher energies than by the axial electric field alone.

In Rockwood's formulation of Boltzmann's equation, the Joule heating term accounts for the divergence of the flux of electrons in energy space resulting from acceleration by the electric field.[24] This can be more simply seen by rewriting the Joule heating term of Eq. (1) as

$$\frac{\partial f(\epsilon,r)}{\partial t}=-\frac{\partial}{\partial\epsilon}\left[\frac{1}{3}\cdot[\mathbf{j}(\epsilon)\cdot\mathbf{E}]\left(1-\frac{2\epsilon}{f}\cdot\frac{\partial f(\epsilon,r)}{\partial e}\right)\right],$$

$$j(\epsilon)=\frac{e^2 f(\epsilon,r)\mathbf{E}(r)}{m_e\nu(\epsilon,r)}, \tag{3}$$

where $\nu(\epsilon,r)$ is the momentum-transfer collision frequency, and $j(\epsilon)$ is the local energy-resolved current density obtained using the local electric field. When written in this form, the contribution of the ambipolar electric field to the energy balance can be accounted for by including both the axial and radial components of the current density and electric field in the dot product of Eq. (3). That is,

$$\mathbf{j}\cdot\mathbf{E}=(jE)_z+(jE)_r, \tag{4a}$$

$$E_r=E_a,\quad j_r=q\cdot D(\epsilon,r)\nabla_r f(\epsilon,r)+\mu(\epsilon,r)E_a f(\epsilon,r). \tag{4b}$$

In Eq. (4), the radial current density contains both advective and diffusion terms. Diffusion of electrons "against" the ambipolar field results in negative Joule heating, or cooling. This term conceptually accounts for the energy transferred from electrons accelerated by the axial electric field to ions accelerated by the radial ambipolar field. The advective term of Eq. 4(b) accounts for positive Joule heating of the electrons by the ambipolar field. Should energy-resolved advection in the ambipolar field dominate over diffusion a given portion of the EED may, in fact, be heated by the ambipolar field while another portion is cooled. Our final form of Boltzmann's equation is then

$$\frac{\partial f(\epsilon,r)}{\partial t}=-\frac{\partial}{\partial\epsilon}\left[\frac{1}{3}\cdot(\mathbf{j}\cdot\mathbf{E})\left(1-\frac{2\epsilon}{f}\cdot\frac{\partial f(\epsilon,r)}{\partial\epsilon}\right)\right]+\left(\frac{\partial f(\epsilon,r)}{\partial t}\right)_c+\nabla_r\cdot[D(\epsilon,r)\cdot\nabla_r f(\epsilon,r)+\mu(\epsilon,r)\cdot\mathbf{E}_a(r)f(\epsilon,r)]. \tag{5}$$

The radial ambipolar field can be approximated by requiring that the local radial flux of ions be equal to the radial flux of electrons. This leads to the well-known expression for the ambipolar field,

$$E_a(r)=\frac{D_e\cdot\nabla_r N_e-D_I\nabla_r N_I}{\mu_e N_e+\mu_I N_I}, \tag{6}$$

where the subscripts e and I denote electrons and ions, D and μ are the swarm-averaged diffusion coefficient and mobility at location r, and N is a density. In our model, the swarm-averaged quantities are calculated by integrating over the spatially resolved EED and we obtain

$$E_a(r)=\frac{\int_0^\infty\mathbf{D}(\epsilon,r)\cdot\nabla_r f(\epsilon,r)d\epsilon-\mathbf{D}_I\nabla_r N_I}{\mu_I N_I+\int_0^\infty\mu(\epsilon,r)f(\epsilon,r)d\epsilon}, \tag{7}$$

where $D(\epsilon,r)$ and $\mu(\epsilon,r)$ are the electron-energy-resolved diffusion coefficient and mobility, respectively. These energy-resolved transport coefficients are approximated as

$$D(\epsilon,r)=\frac{2}{3}\cdot\frac{\epsilon}{m_e\nu(\epsilon,r)},\quad \mu(\epsilon,r)=\frac{q}{m_e\nu(\epsilon,r)}, \tag{8}$$

where m_e is the electron mass and ν is the energy-resolved momentum-transfer collision frequency. At sufficiently low pressures and high energies, the apparent thermal-diffusion velocity may exceed the thermal velocity v_t. In these cases, $D(\epsilon,r)$ is restricted to the smaller of the value in Eq. (8) and $\Lambda\cdot v_t$, where Λ is the local diffusion length.

The self-sustaining, steady-state E/N was obtained by finding that value which balances the volumetric rate of ionization with the rate of electron loss to the wall. This is obtained by assuming no volumetric recombination and solving

$$\int\int f(\epsilon,r)\left(\frac{2\epsilon}{M_e}\right)^{1/2}\sum_i\sigma_i(\epsilon)d\epsilon\,2\pi r\,dr=\int[D(\epsilon)\nabla_r f(\epsilon,R)+\mu(\epsilon)f(\epsilon,R)E_a(R)]2\pi R\,d\epsilon, \tag{9}$$

where R is the radius of the discharge tube.

Our method for obtaining $f(\epsilon,r)$ is to directly integrate Eq. (5) in time until the distribution reaches a steady state. Computationally, the Joule heating and collision terms were expressed in the same fashion as Bretagne, Go-

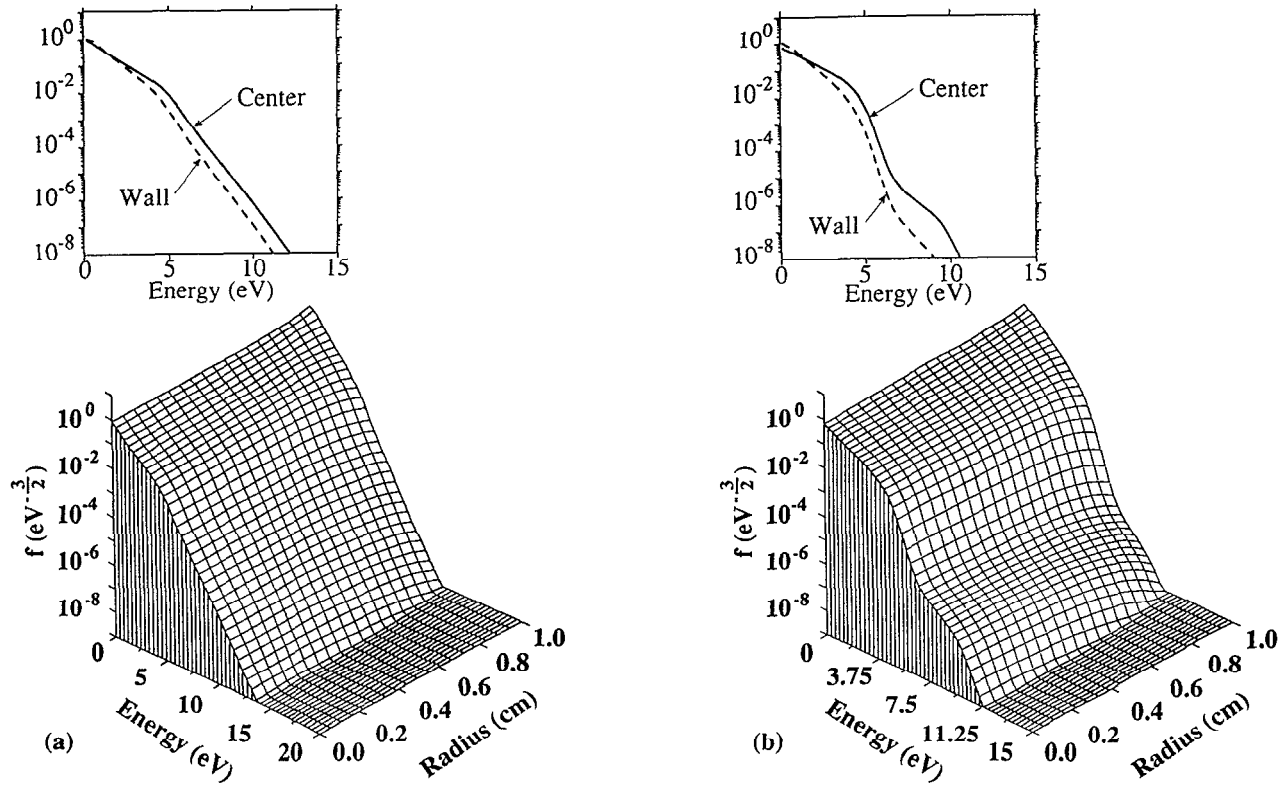

FIG. 1. The electron energy distribution (EED) as a function of radius, calculated using the fully coupled scheme: (a) 1 Torr and (b) 3 Torr. The distributions are separately normalized at each radial point. The insets show the EED at the center of the discharge and at the wall.

dart, and Puech,[25] which was itself an implementation of Rockwood's method.[24] Electron-electron collision terms were implemented in the same fashion. The spatial transport terms were couched using finite differences and the donor cell method. The boundary conditions are that spatial derivatives are zero on the axis and all densities are zero at the wall. Although the latter boundary condition is not strictly true in some cases, as discussed by Metze, Ernie, and Oskam,[26] the deviation is small and does not substantially affect our results. The system of equations was integrated using a third-order Runga–Kutta technique with adaptive step size. We typically used 15–20 radial cells and 40–60 energy cells in our calculations.

III. RADIALLY RESOLVED ELECTRON ENERGY DISTRIBUTIONS

In this section, we will discuss results for radially resolved EEDs obtained with our model. Since the original motivation in developing this model was to address issues related to Hg lasers and fluorescent lighting sources, our sample systems use rare-gas/Hg mixtures. The base case uses conditions that are typical for a pulsed recombination Hg laser discharge. The cylindrical discharge tube has a diameter of 1.0 cm and a gas fill of He/Hg=93/7. The cross sections for electron collisions with the mercury ground state were obtained from Rockwood.[24] The electron momentum-transfer cross section for He was obtained from Hayashi,[27] while the excitation cross sections were taken from Bouef and Marode.[28] The ionization cross section for He was obtained from Rapp and Englander-Golden.[29] Mobilities for Hg^+ and He^+ in He and Ar, as given by Ellis *et al.*,[30] were used to determine the radially resolved ambipolar field. Electron-electron collisions were included in the calculations in the manner discussed above.

Radially resolved EEDs obtained for full coupling are shown in Fig. 1 for total gas pressures of 1 and 3 Torr. [By full coupling, we refer to calculations that include all of the terms in Eq. (5).] The ambipolar potentials obtained by integrating the radial ambipolar electric field for each case (including 10 Torr) are shown in Fig. 2. To include the effects of superelastic and multistep processes in the calculation we specified that the metastable Hg density is $[Hg^*]/N=10^{-5}\cos(\pi r/2R)$. These densities are commensurate with those found in rare-gas–Hg positive-column discharges.[31] For comparison, EEDs calculated for the same conditions while using the LFA (that is, ignoring radial transport and joule heating by the ambipolar field) are shown in Fig. 3. The EEDs in the figure are separately normalized at each radial point. For these cases, we assumed that there was negligible gas heating, so that the gas density profile is uniform. At 1 Torr, the ambipolar E/N adjacent to the wall is 43.6 Td ($1\ \text{Td}=1\times10^{-17}\ \text{V cm}^2$) while the axial E/N is 14 Td. At 3 Torr, the ambipolar E/N adjacent to the wall is 13.9 Td with an axial E/N of 6 Td. In both cases, the ambipolar E/N exceeds that due to the applied electric field.

At 1 Torr, the fully coupled case is depleted of high-energy electrons in the tail of the EED across the radius

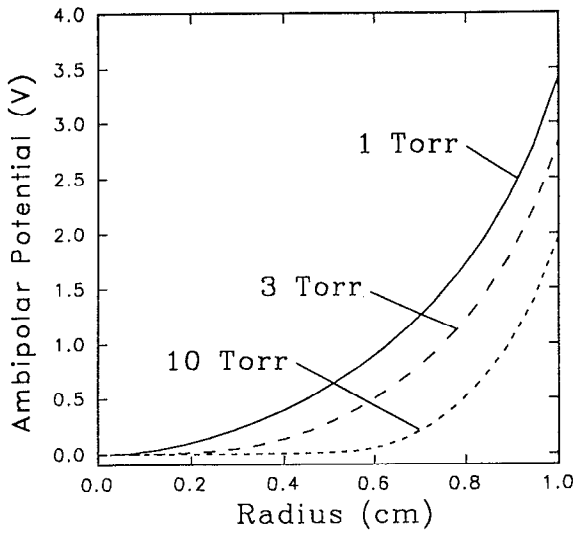

FIG. 2. Calculated ambipolar potentials for fully coupled cases obtained by integrating the ambipolar electric field. The conditions are the same as in Fig. 1.

compared to that using the LFA. This depletion results from the diffusion of high-energy electrons (which have longer mean free paths) against the field to the wall. The depletion is somewhat more severe near the wall. The EED shows evidence of being cut off approximately at the ambipolar potential, as predicted by Tsendin and Golubovskii.[16] The effect of the space-charge field, increasing toward the wall, is to decelerate the electron flux relative to the LFA case. This increases the thermal portion of the EED near the wall. Due to the high self-sustaining E/N, the effects of energy loss due to electronic excitation of Hg and energy gain due to superelastic relaxation are not as readily apparent in the fully coupled case, although they can be seen in the LFA case.

At 3 Torr, the same trends as in the 1 Torr case can be seen, though not to as great an effect. Since the electron mean free paths are shorter, the diffusion cooling effect is less pronounced. The electron flux is, though, still decelerated by the ambipolar electric field, creating a large thermal component by the wall. The self-sustaining E/N is lower at 3 Torr and therefore the effect of energy loss and gain by excitation and superelastic collisions can be more readily seen. The EED is cut off at approximately 5 eV commensurate with the inelastic threshold for exciting the Hg(^1P) states. Superelastic relaxation of those states by the numerous thermal electrons increases their energy by the same 5 eV. The result is that an increase in the tail of the distribution above 5 eV, somewhat "mirroring" the thermal distribution. The superelastically heated tail of the EED is nearly constant as a function of radius at inner radii when using the LFA, while that of the fully coupled case begins to show evidence of diffusion cooling.

Recall that the Hg(^1P) density was specified to have a cosine profile, which falls steeply at the wall. This distri-

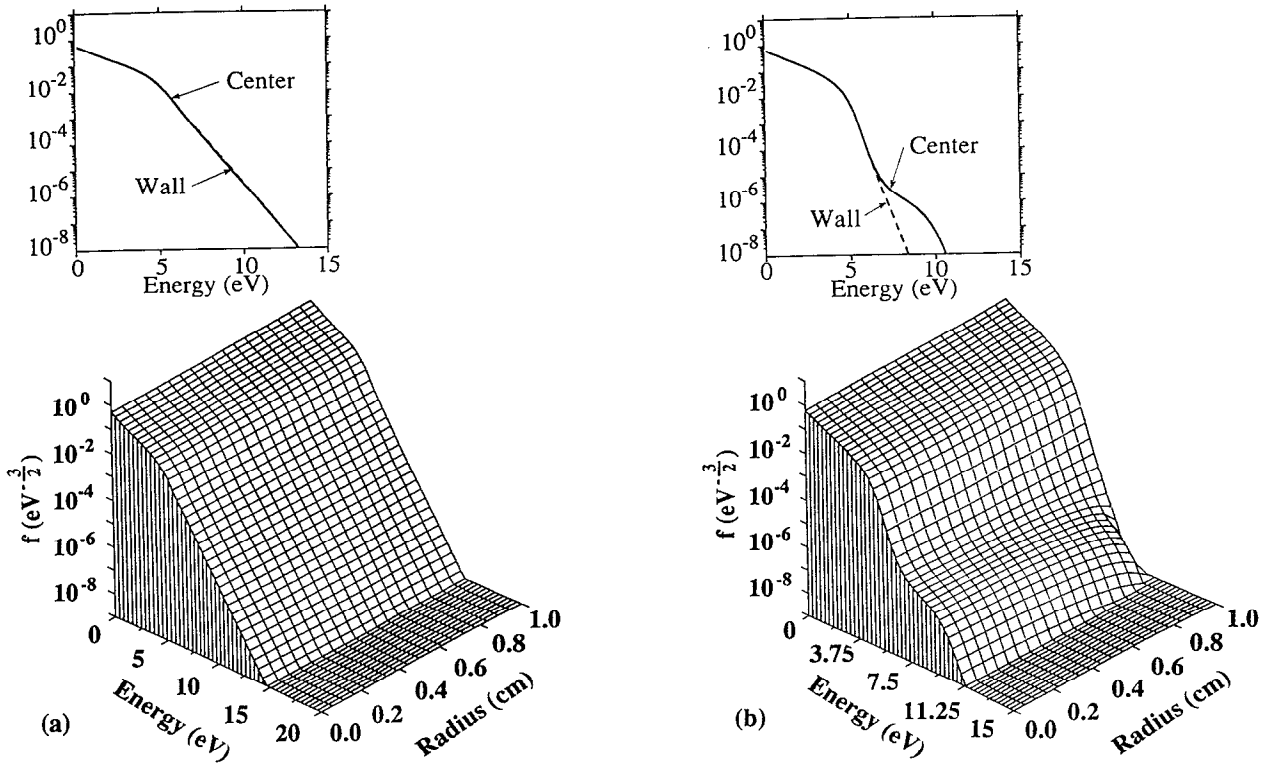

FIG. 3. The EED as a function of radius calculated using the local-field approximation (LFA) for the same conditions as in Fig. 1: (a) 1 Torr and (b) 3 Torr. The insets show the EED at the center of the discharge and at the wall. The EEDs at 1 Torr are nearly uniform as function of radius in spite of the differences in superelastic heating. At 3 Torr the EED near the wall is depleted of superelastically heated electrons.

bution causes a depletion of the superelastically heated electrons near the wall in both the LFA and fully coupled cases. In the LFA case, the superelastically heated tail is nearly absent at the wall, while in the fully coupled case the tail at the wall persists to a greater degree. This effect results from radial transport of superelastically heated electrons at inner radii towards the wall.

The radially dependent EED is determined by convection in both coordinate (i.e., r) space and velocity space. The degree to which convection in velocity space caused by the ambipolar electric field affects the EED is shown in Fig. 4. In this figure, we show the EED for 3 Torr when we included electron drift and diffusion in the ambipolar electric field; however, the Joule heating (or cooling) terms have been neglected. Note that the distribution is depleted of electrons at energies below the inelastic threshold near the wall. This effect is due to the drift of these electrons back toward the axis in the ambipolar field at a faster rate than elastic momentum-transfer collisions are able to advect electrons down the energy axis. Below the inelastic threshold, advection down the energy axis is a slow process because it proceeds at a fractional rate of only $2m_e/M$ per collision. The cooling of the superelastically heated tail near the wall is also diminished relative to the center of the discharge. This implies that the effects of diffusion cooling can be averaged over the bore of the discharge whereas the dominant cooling effect near the wall results from energy exchange with the ambipolar field.

Electron temperatures ($T_e = \frac{2}{3}\langle\epsilon\rangle$) as a function of radius for the 1 Torr case described above, and a similar calculation at a pressure of 10 Torr (self-sustaining $E/N = 3.5$ Td), appear in Fig. 5. As expected, when using the LFA the electron temperature is uniform as a function of radius since the E/N is uniform across the bore. The effect of superelastic heating on the bulk electron temperature is nominal. When including convection (drift and diffusion) but excluding the ambipolar Joule heating (or cooling), the electron temperature is reduced on the axis and increased near the wall relative to the LFA case. The decrease near the axis results from a spatially averaged loss of higher-energy electrons to the absorbing wall, resulting in the lower average energy. The increase in the local electron temperature near the wall results from the depletion of low-energy electrons by drift away from the wall in the high ambipolar field, as shown in Fig. 4. Similar effects are predicted by Bernstein and Holstein[12] and others.[15–17] When fully resolving the EEDs, the calculated electron temperature is lowered throughout the volume. The reduction in temperature near the axis is due to the diffusion of high-energy electrons as described above. The weak maximum in T_e near 0.5 cm indicates some small amount of diffusion heating (see below). Near the wall, the decrease is dominantly due to Joule "cooling" which occurs when electrons diffuse against the ambipolar field. At 10 Torr, the distribution-averaged effects of diffusion heating are absent and T_e monotonically decreases towards the wall as the ambipolar field increases.

Recalling that low-energy electrons, which are far more numerous, have a higher rate of momentum transfer

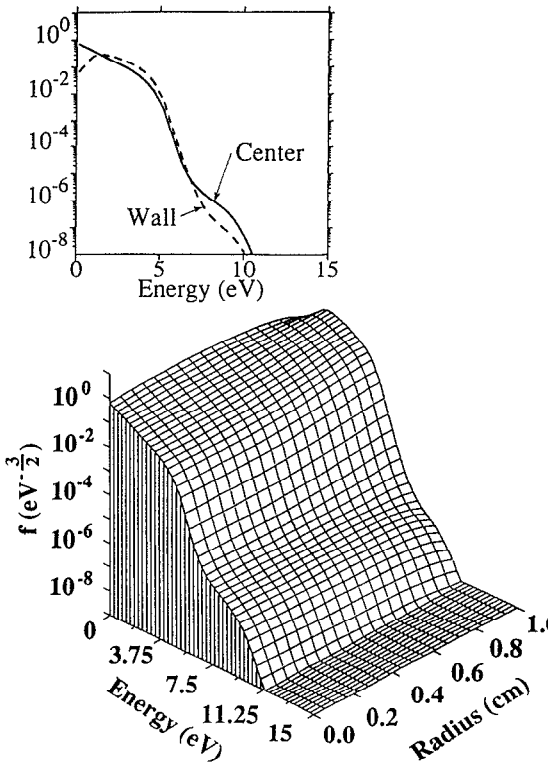

FIG. 4. The EED as a function of radius obtained while including electron diffusion and drift, but excluding Joule heating by the ambipolar field. The inset shows the EED at the center of the discharge and at the wall. The electron density near the wall is depleted of low-energy electrons due to advection in the large ambipolar fields.

than high-energy electrons, the LFA is a more accurate description for their transport. Since the magnitude of the local field is higher near the wall, one might expect that the temperature would increase there as well. As we saw, however, the dominant direction of transport by diffusion is against the field, and hence there is cooling. Since the higher-energy electrons do not obey the LFA, there should be no expectation that rate coefficients having high-energy thresholds will scale in a similar fashion as a function of radius as does T_e. The effects of electron transport and joule heating by the ambipolar field are, perhaps, most telling on the rate coefficients for excitation and ionization for processes having high-energy thresholds.

The rate coefficient for ionization of the Hg ground state, normalized to its maximum value, is shown in Fig. 6(a) as a function of radius using the LFA and in Fig. 6(b) using the fully coupled method. The rate coefficients obtained using the LFA generally decrease across the radius, reflecting the decreasing contribution of superelastically heated tail electrons. When allowing for radial transport, the rate coefficients for ionization also decrease across the radius. There is a smaller decrease near the wall in the fully coupled case. At smaller radii, we see the effects of diffusion and Joule cooling. At larger radii, we see the effects of mixing of the superelastically heated electrons as a function of radius which heats the distribution above the inelastic threshold. These trends are more clearly seen in

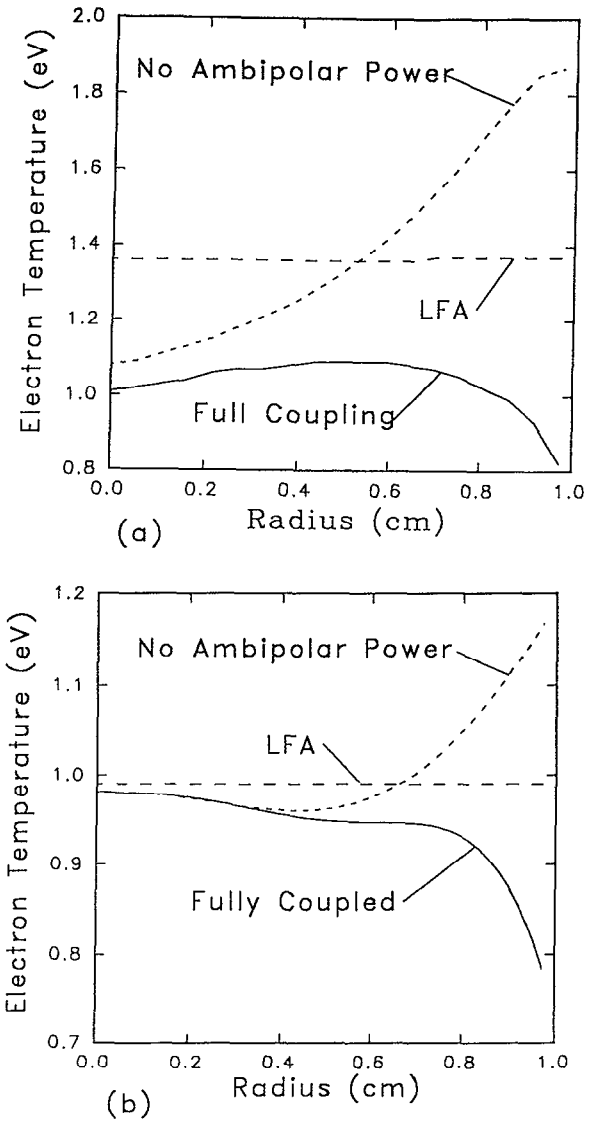

FIG. 5. The electron temperature at (a) 1 Torr and (b) 10 Torr. Results are shown for the local-field approximation (LFA), full coupling, and when excluding the Joule heating due to the ambipolar electric fields. Whereas the LFA case does not vary across the radius, including only electron drift and diffusion artificially heats the distribution near the wall. By adding ambipolar Joule heating, the distribution is cooled near the wall by the exchange of energy between the electrons and the ambipolar field.

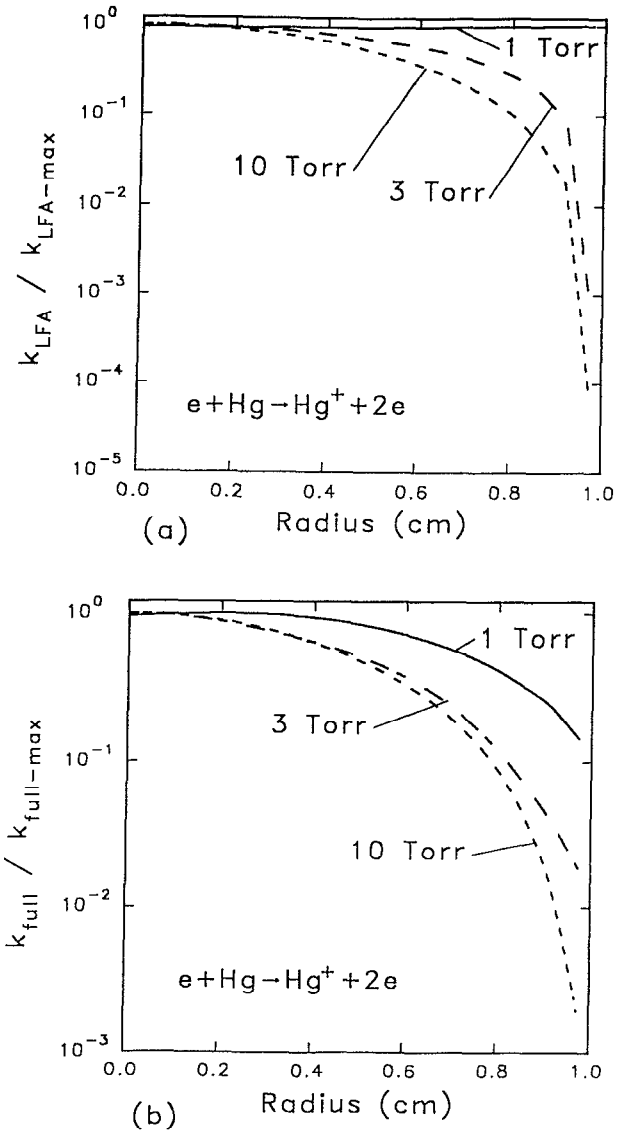

FIG. 6. Ionization rate coefficients for ground-state Hg as a function of radius at different pressures calculated using (a) the LFA and (b) the full coupled scheme. The rate coefficients have been normalized by their maximum values on the axis. The decrease in rate coefficients in the LFA case results from a lower rate of superelastic heating. That in the fully coupled case results largely from ambipolar cooling.

Fig. 7 where the rate coefficients for ionization and excitation are normalized by their values obtained using the LFA. In the case of excitation of Hg(^1P), the rate coefficients uniformly decrease relative to their LFA values due to diffusion cooling effects. The ionization rate coefficients, which are more responsive to the tail of the EED, behave differently. The rate coefficients generally decrease relative to the LFA values, more so at low pressure. The rate coefficient, though, increases relative to the LFA value near the wall at higher pressures. This results from the radial transport of high-energy superelastically heated electrons into a region near the wall where the excited-state density is lower and the local rate of superelastic heating is lower.

To discern which of these effects, (transport losses or Joule heating/cooling) are dominantly responsible for the observed change in rate coefficients relative to using the LFA, the following computer experiment was performed. The radially dependent EED was calculated while including the transport terms in Eq. (8) but excluding radial Joule heating. These rate coefficients were used to normalize the values obtained using the fully coupled case and the results are shown in Fig. 8. The effects of Joule cooling are larger at lower pressures where the ambipolar fields and electron temperatures are higher. For these conditions, the dominant cooling effect appears to be the interaction of electrons with the ambipolar field. The cooling effects are more localized near the wall where the ambipolar field is

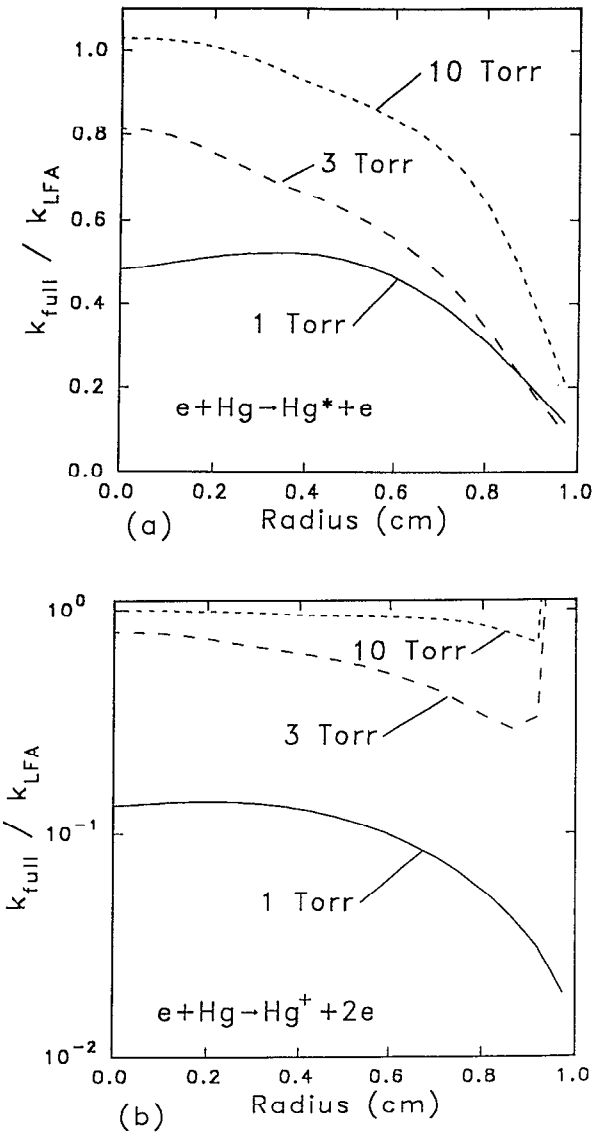

FIG. 7. Rate coefficients for electron impact on Hg obtained using the fully coupled scheme normalized by their values using the LFA: (a) excitation and (b) ionization. Enhancements in the ionization coefficients near the wall relative to the LFA results from the lack of superelastically heated electrons at those locations using the LFA.

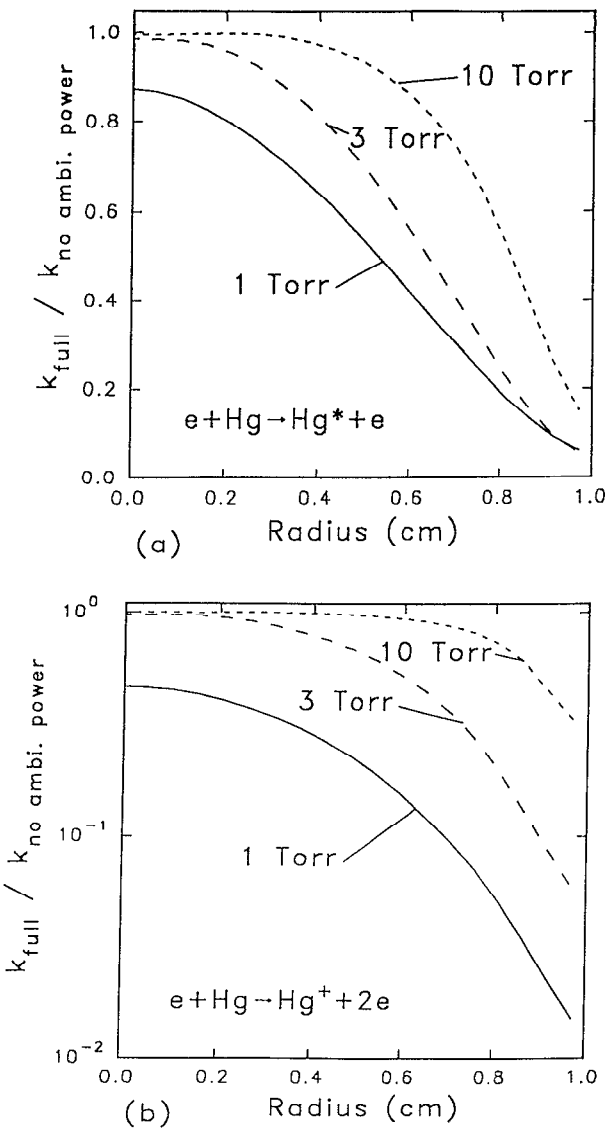

FIG. 8. Rate coefficients for electron impact on Hg obtained using the fully coupled scheme normalized by their values obtained while excluding heating/cooling by the ambipolar electric fields: (a) excitation and (b) ionization.

large at higher pressure due to the reduced amount of radial mixing of the EED.

The consequence of radial transport in the EED on excited states in the fluorescent lamp were investigated for the conditions of Dakin and Bigio.[31] In their article, absolute measurements of densities of the Hg(^3P) manifold were reported for Ar/Hg mixtures. The fill pressure of the buffer gas was 2.81 Torr Ar, the gas temperature was 313 K, dc current was 400 mA, and the tube radius was 1.7 cm. In our model we included an effective metastable state, Hg*, which is the degeneracy-weighted combination state of the ^3P manifold assuming rapid mixing. We also included an effective higher-lying excited state, Hg**, representing 17 Hg I levels.[32] The cross sections used for excitation of Hg* were taken from Rockwood.[24] The excitation and ionization cross sections for the Hg** state from the ground and Hg* states were obtained from the generalized formulas found in Drawin.[33] An effective lifetime for Hg* which takes into account radiation trapping was calculated from van de Weijer and Cremers,[34] and was found to be 7.5 μs. Diffusion coefficients for Hg atoms were calculated from expressions found in Hirschfelder, Curtiss, and Bird.[35] Partial differential equations including electron-impact excitation and quenching, heavy particle reactions, radiative relaxation, and transport by diffusion were couched in finite difference form using the donor cell method. The system of equations were implicitly solved using an iterative matrix inversion technique.

The densities of Hg* calculated as a function of radius obtained using the fully coupled scheme and neglecting ambipolar Joule heating are shown in Fig. 9(a) together with the experimentally determined values.[31] Both ap-

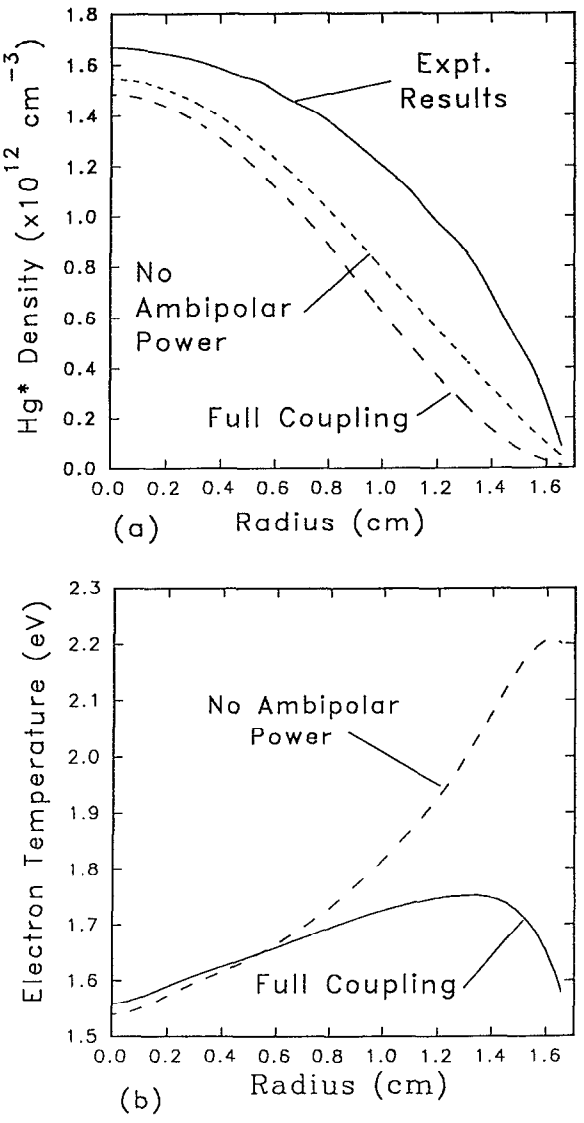

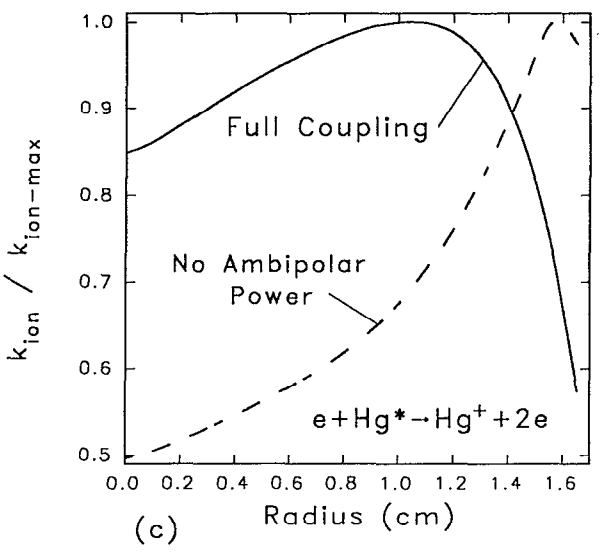

FIG. 9. Discharge parameters for a cylindrical positive column discharge in an Ar/Hg gas mixtures similar to the fluorescent lamp studied by Dakin and Bigio (Ref. 31). (a) Density for our Hg* obtained using the fully coupled method, excluding the effects of ambipolar power and experimental values obtained by Dakin and Bigio. (b) The electron temperature and (c) rate coefficient for electron-impact ionization of Hg* normalized by its maximum value.

proaches yield densities comparable to values obtained in the experiment with a moderate depletion of the calculated densities at larger radii. This disagreement may be attributed to our poor representation of radiation transport or neglecting rarification due to gas heating. When excluding the terms for the ambipolar power, the predicted Hg* density is somewhat larger than that for the fully coupled case. The predicted electron temperature and normalized metastable ionization rate coefficient for these cases are shown in Figs. 9(b) and 9(c). In the absence of Joule cooling by the ambipolar field, the electron temperature and rate coefficients increase near the wall due to the depletion of low-energy electrons by the ambipolar field. In the fully coupled cases, Joule cooling more than compensates for the advection of low-energy electrons away from the wall. Small maxima in both the electron temperature and rate coefficient are observed at intermediate radii in the fully coupled case, an effect we attribute to some amount of diffusion heating of the lower portion of the distribution.

IV. COMPARISON WITH PREVIOUS WORKS

As briefly discussed in Sec. I, the effects of space-charge fields and transport on the EED in cylindrical bore discharges have been previously addressed by others. One of the first works was by Bernstein and Holstein.[12] Their treatment addressed conditions where the radial electric fields are much larger than the applied axial field. With this assumption, and the approximation that the loss of electrons to the wall is not important to the EED, they found a net higher rate of ionization on the axis of the discharge than one would obtain using the LFA. This is a consequence of the trapping of the electrons by the space-charge field. Electrons generated in high-space-charge regions by ionization are accelerated toward the axis by the ambipolar field, gaining a large fraction of the space charge potential. This condition requires that the plasma be largely collisionless. However, when the applied axial field is comparable to the ambipolar field, and the loss of electrons to the wall is significant, other scalings may result.

To demonstrate these effects we performed the following computer experiment. The EED was computed while excluding transport to the wall but including all other processes. The ambipolar field for this case was obtained from the fully coupled example. The Hg ionization rate coefficient (normalized by that value obtained from a fully coupled case that includes transport to the wall) is plotted as a function of radius in Fig. 10(a) and the electron temperature is shown in Fig. 10(b). While the assumption that there is no transport to the wall makes little difference at 10 Torr, the ionization rate is larger at 1 Torr when losses to the wall are ignored. Electrons at the lower pressure sample a larger fraction of the volume, and hence losses at the wall impact a larger fraction of the ionization processes. Of the increase in electron temperature near the wall relative to the fully coupled case, approximately half is due to the retention of electrons which would have otherwise been lost to the wall, and half is due to additional heating of those electrons by the imposed ambipolar field.

Tsendin[14] examined the effects of an inhomogeneously electric fields on the EED in a positive column. Tsendin considered electron diffusion in both space and energy as well as electron drift in a transverse electric field. The solution yielded a radial dependence for the electron temperature which decreased across the axis, in agreement with our results. Tsendin also found a pooling of the electron density at the axis, resulting from the potential well formed by the space charge. He excluded, however, the loss of electrons to the wall of the discharge tube. Zhilinskii and co-workers,[15] later considered the loss of electrons to the wall, and the resulting diffusion cooling. This effect was more pronounced at low pressures due to a decrease in the wall potential resulting from a significant depletion of tail electrons in the EED. He suggested that diffusion cooling is dominated by the work performed by the electrons in opposing the ambipolar forces in the plasma column as we found here.[15]

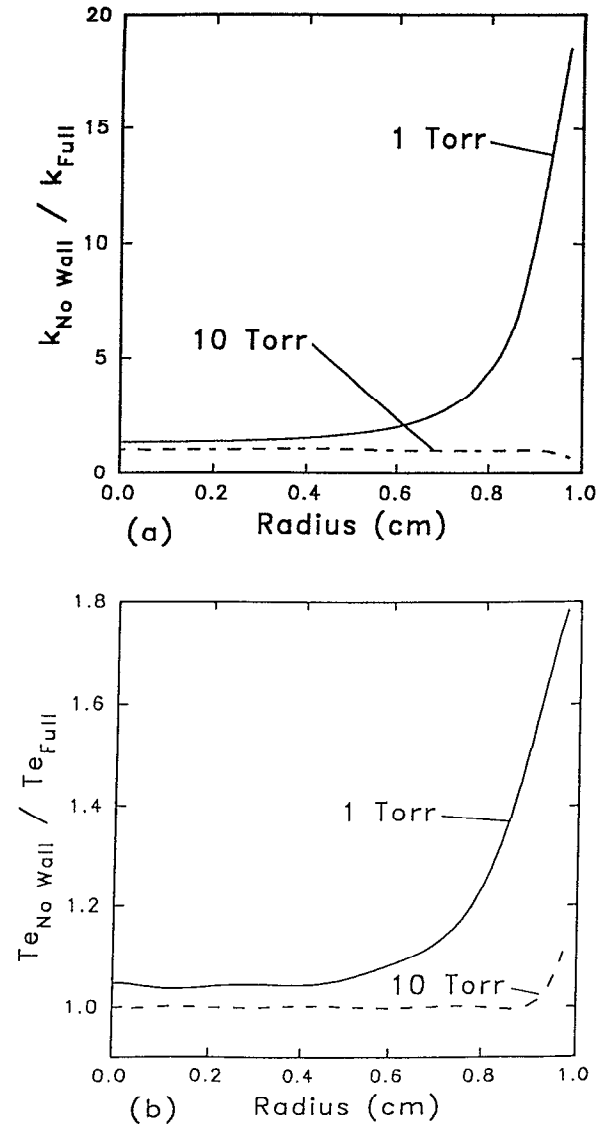

FIG. 10. Results of a computer experiment where electron flux to the wall is ignored: (a) rate coefficient for ionization and (b) electron temperature. These coefficients and temperatures have been normalized by their values obtained from the fully coupled case. The ambipolar electric field for the case where electron flux to the wall is ignored was obtained from the fully coupled case. While the higher-pressure case shows little effect of allowing electron losses to the wall, at lower pressure the discharge is heated near the wall relative to the fully coupled case.

V. CONCLUDING REMARKS

A model for the spatially resolved electron energy distribution function has been developed and applied to the cylindrical bore positive column. In this model, the two-term spherical harmonic expansion solution for Boltzmann's equation is augmented by including energy resolved drift and diffusion, and heating/cooling by the ambipolar electric field. We generally find a depletion of the high-energy component of the distribution which results from at least two causes. The first is inelastic collisions with Hg. The second results from diffusion against the ambipolar field, and an enhancement in the thermal portion of the distribution near the wall. These effects are somewhat mitigated by the radial transport of superelastically heated electrons from the axis, where the rate of heating is high, to the wall where the rate of heating is low.

Our method of radially resolving the EED is easily extended to higher pressures. The necessity to do so, though, declines as $p \cdot d$ exceeds 10 Torr cm. The extension of this model to lower pressures, though, is limited by treating electron transport by drift diffusion, particularly at higher energies. At $p \cdot d$ below 0.1 Torr cm, our assumptions become questionable. In these cases, two approaches can be considered. The first is to treat the problem using a fully kinetic approach. The second is to assume that the EED is radially well mixed and use a radially averaged E/N.

Another limitation to this model occurs at low pressures and large ambipolar fields. Recall that the two-term SHE assumes that the electron velocities are nearly isotropic and any directed velocities arising from the electric field are perturbations. In keeping with this approximation, the directed energy resulting from the radial transport should be a small fraction of the particle's energy. We sometimes violate this criterion at low electron energies

($\epsilon < 0.5$ eV) near the wall where the ambipolar electric fields are greatest. This condition will result in slightly higher calculated electron temperatures near the wall. However, the degree to which we violate the isotropic criterion is small enough to be within the range of error already resulting from other assumptions in the model.

A deficiency in the present model is our simple treatment of the transport of ions, whose densities are obtained by assuming quasineutrality. Metze and co-workers[26] solved the radial transport equation and Poisson's equation for the cylindrical bore positive column using ensemble averaged rate coefficients. They found differences between the electron and ion densities on the axis for our conditions of $\simeq 5\%$, and increasing towards the wall to as much as 20%. These differences, though important, do not directly affect our calculation since the ambipolar electric fields obtained using our method do not significantly differ from those obtained by Metze and co-workers.[26]

ACKNOWLEDGMENTS

The authors would like to thank Dr. Arthur Phelps and Dr. James Dakin for their helpful comments and insight. This work was supported by Sandia National Laboratory and the National Science Foundation (Grants No. ECS91-09326 and No. CTS91-13215).

[1] L. H. S. Huxley and R. W. Crompton, *Diffusion and Drift of Electrons in Gases* (Wiley, New York, 1974), and references therein.
[2] S. Yachi, Y. Kitamura, K. Kitamori, and H. Tagashira, J. Phys. D. **21**, 914 (1988).
[3] A. V. Phelps and L. C. Pitchford, Phys. Rev. A **31**, 2932 (1985).
[4] Y. Weng and M. J. Kushner, Phys. Rev. A **42**, 6192 (1990).
[5] M. Surendra, D. B. Graves, and I. J. Morey, Appl. Phys. Lett. **56**, 1022 (1990).
[6] M. Surendra, D. B. Graves, and G. M. Jellum, Phys. Rev. A **41**, 1112 (1990).
[7] T. J. Sommerer, W. N. G. Hitchon, and J. E. Lawler, Phys. Rev. Lett. **63**, 2361 (1989).
[8] M. J. Kushner, Trans. Plasma Sci. **19**, 387 (1991).
[9] J. H. Ingold, in *Gaseous Electronics*, edited by M. N. Hirsh and H. J. Oskam (Academic, New York, 1978), Vol. I, Chap. 2, p. 37.
[10] W. P. Allis and D. J. Rose, Phys. Rev. **93**, 84 (1954).
[11] B. N. Ganguly and A. Garscadden, Appl. Phys. Lett. **46**, 540 (1985).
[12] I. B. Bernstein and T. Holstein, Phys. Rev. **94**, 1475 (1954).
[13] J. L. Blank, Phys. Fluids **11**, 1686 (1968).
[14] L. D. Tsendin, Sov. Phys. JETP **39**, 805 (1974).
[15] A. P. Zhilinskii, I. F. Livintseva, and L. D. Tsendin, Sov. Phys. Tech. Phys. **22**, 177 (1977).
[16] L. D. Tsendin and Y. B. Golubovskii, Sov. Phys. Tech. Phys. **22**, 1066 (1977).
[17] N. A. Vorob'eva, V. M. Milenin, and L. D. Tsendin, Sov. Phys. Tech. Phys. **24**, 442 (1979).
[18] A. V. Phelps, J. Res. Nat. Inst. Stand. Technol. **95**, 407 (1990).
[19] A. K. Bhattacharya and J. H. Ingold, J. Appl. Phys. **43**, 1535 (1972).
[20] C. M. Ferreira and A. Ricard, J. Appl. Phys. **54**, 2261 (1983).
[21] M. A. Biondi, Phys. Rev. **93**, 1136 (1954).
[22] D. Smith, A. G. Dean, and N. G. Adams, Z. Phys. **253**, 191 (1972).
[23] J. Boulmer, C. Sol., and J. C. Gauthier, Phys. Lett. A **41**, 83 (1972).
[24] S. D. Rockwood, Phys. Rev. A **8**, 2348 (1973).
[25] J. Bretagne, J. Godart, and V. Puech, J. Phys. D Appl. Phys. **15**, 2205 (1982).
[26] A. Metze, D. W. Ernie, and H. J. Oskam, Phys. Rev. A **39**, 4117 (1989).
[27] M. Hayashi, Report No. IPPJ-AM-19, Nagoya Institute of Technology, 1982.
[28] J. P. Bouef and E. Marode, J. Phys. D **15**, 2169 (1982).
[29] D. Rapp and P. Englander-Golden, J. Chem. Phys. **43**, 1464 (1965).
[30] H. W. Ellis, R. Y. Pai, E. W. McDaniel, E. A. Mason, and L. A. Viehland, At. Data Nucl. Data Tables **17**, 177 (1976).
[31] J. T. Dakin and L. Bigio, J. Appl. Phys. **63**, 5270 (1988).
[32] W. L. Wiese and G. A. Martin, *Wavelengths and Transition Probabilities for Atoms and Atomic Ions*, Nat. Bur. Stand. Ref. Data Ser., Nat. Bur. Stand. (U.S.) Circ. No. 68 (U.S. GPO, Washington, DC, 1980), Part II.
[33] H. W. Drawin, EUR-CEA-FC-383, 1967.
[34] P. van de Weijer and R. M. M. Cremers, J. Appl. Phys. **57**, 672 (1985).
[35] J. O. Hirschfelder, C. F. Curtiss, and R. B. Bird, *Molecular Theory of Gases and Liquids* (Wiley, New York, 1954), p. 539.